09/06/2021

Higgs boson couplings to bosons with the ATLAS experiment

Luca Franco
(on behalf of the ATLAS collaboration)

Higgs couplings

- The Standard Model (SM) lagrangian:

$$\mathcal{L} = -\frac{1}{4} F_{\mu\nu} F^{\mu\nu}$$

$$+ i \bar{\psi} \not{D} \psi + h.c.$$

$$+ \bar{\psi}_i y_{ij} \psi_j \phi + h.c.$$

$$+ |D_\mu \phi|^2 - V(\phi)$$

Higgs couplings to fermions (see Tristan‘s talk)

Higgs couplings to bosons (covered by this talk)

Higgs self-coupling (partially covered)

N_H : Nr of expected Higgs bosons @139fb^{-1}

Higgs bosonic decays

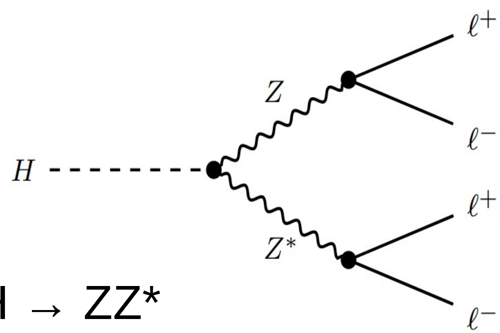

H → ZZ*
BR: 2.6 %
N_H ~ 200k

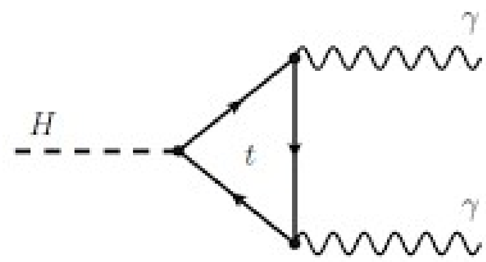

H → γγ
BR: 0.2 %
N_H ~ 14k

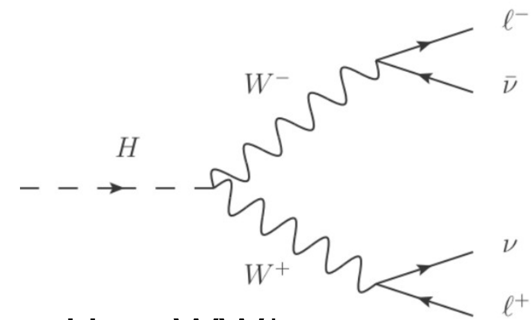

H → WW*
BR: 21.4 %
N_H ~ 150M

- Crucial channels for Higgs discovery in Run 1;
- Allow accurate measurements of the Higgs properties in various regions of the phase space during Run 2;
- Profit from the full Run 2 dataset → 139fb^{-1} of pp collisions at $\sqrt{s}$=13 TeV.

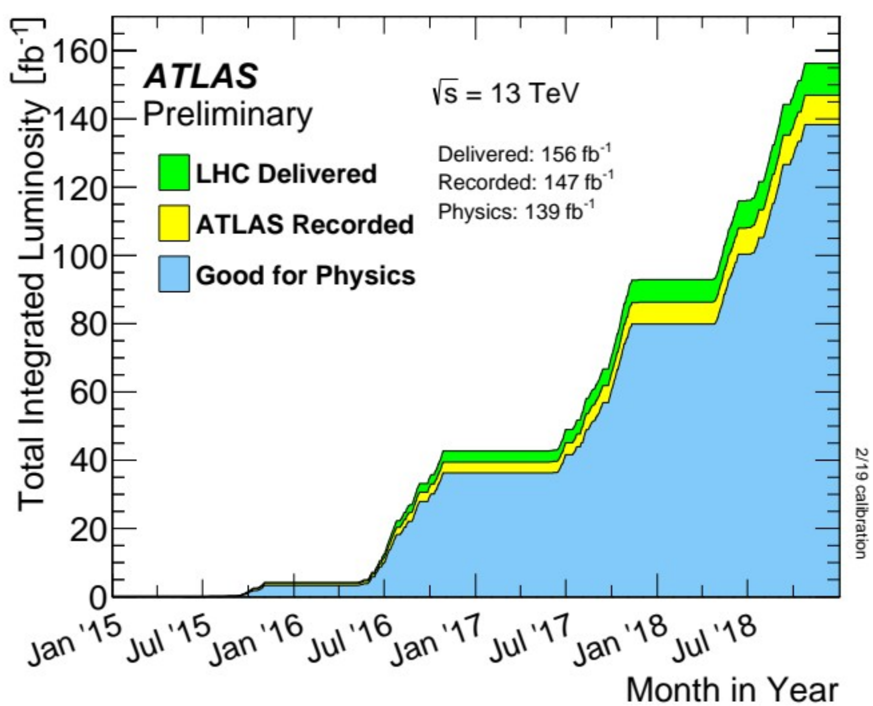

Higgs production modes

- % of total production cross section (XS) at mH=125.09 GeV and √s=13 TeV in pp collisions:

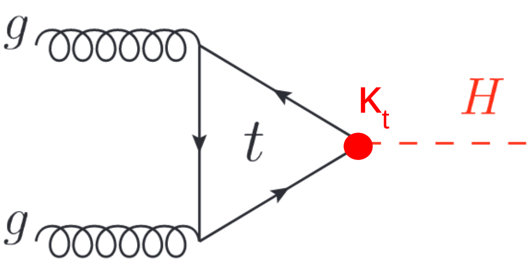

Gluon fusion (ggF)
87%

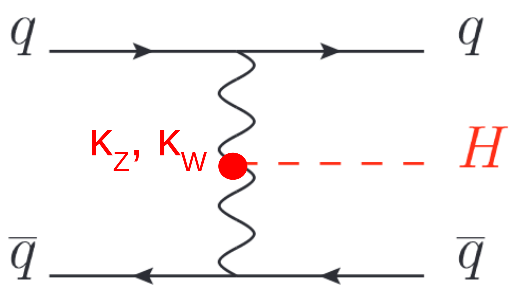

Vector boson fusion (VBF)
6.8%

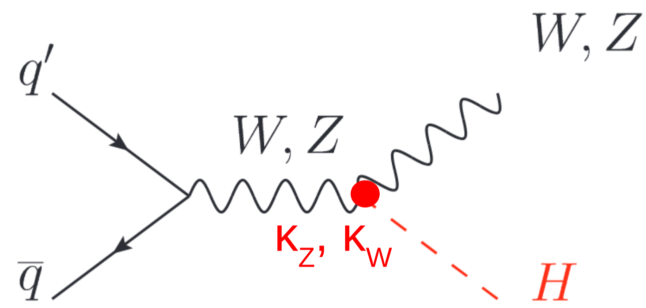

Associated vector boson (VH)
4%

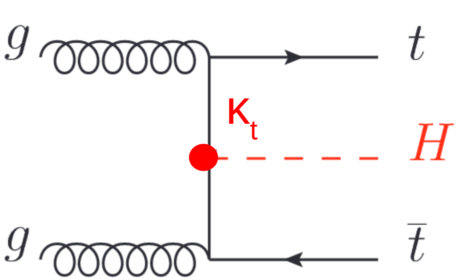

Associated top quark pair (ttH)
0.9%

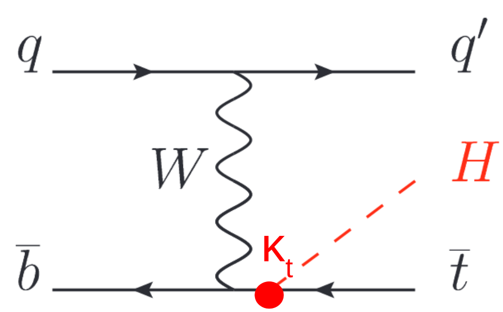

Associated single top (tH)
<0.1%

- Coupling strengths can be probed through the production rate of different mechanisms.

Simplified Template Cross Sections

- Measurements performed in the bins proposed by the STXS stage 1.2 framework:
  - Minimize theoretical uncertainties;
  - Maximize experimental sensitivities;
  - Separately measure regions of phase space potentially sensitive to BSM effects;
  - Ease combination with other decay channels.

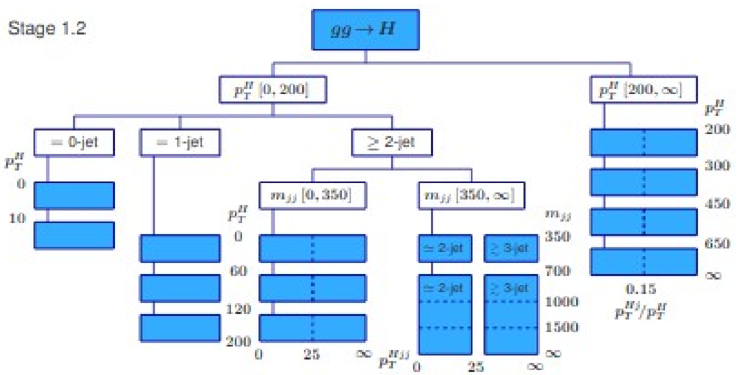

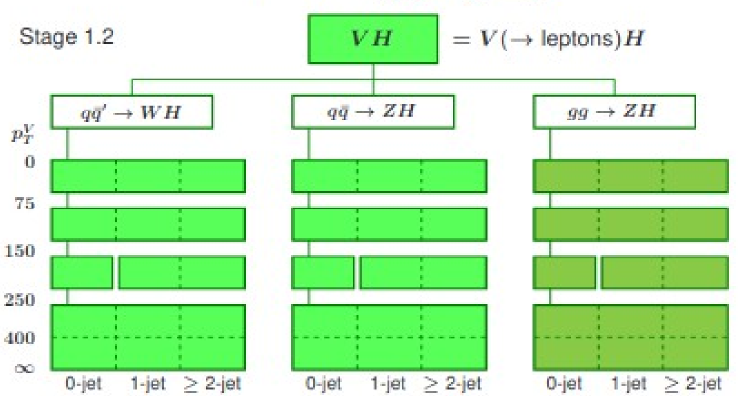

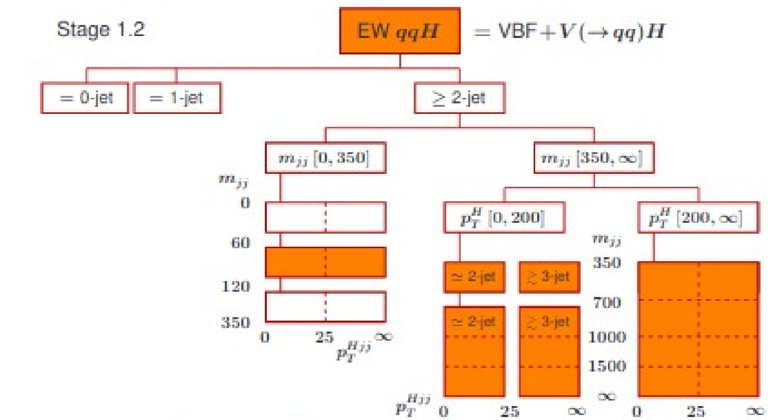

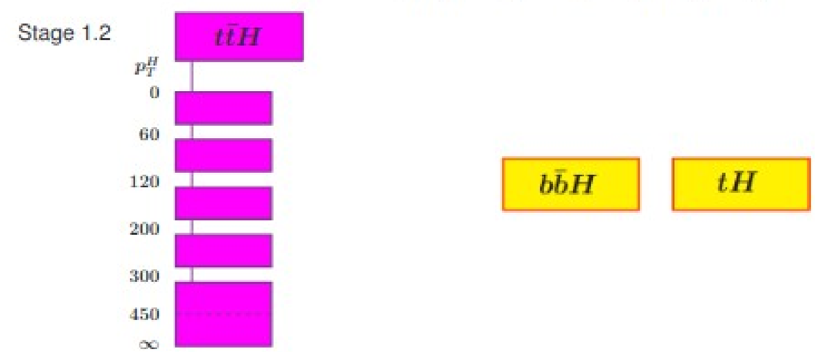

H→γγ: prod. mode XS

- Measurements of total XS, production modes and STXS (27 regions);
- Multiclass Boosted Decision Tree (BDT) to categorize events following STXS definition minimizing misidentification rates;
- Binary BDT to separate signal from background in each category;
- Fit the Higgs narrow peak over the SM falling background in $m_{\gamma\gamma}$ using analytic functions;
- Systematic uncertainties similar to statistical ones in ggF (background modeling) and VBF (parton shower modeling).

$$(\sigma \times B_{\gamma\gamma})_{\rm obs} = 127 \pm 10 \text{ fb}$$

$$(\sigma \times B_{\gamma\gamma})_{\rm exp} = 116 \pm 5 \text{ fb}$$

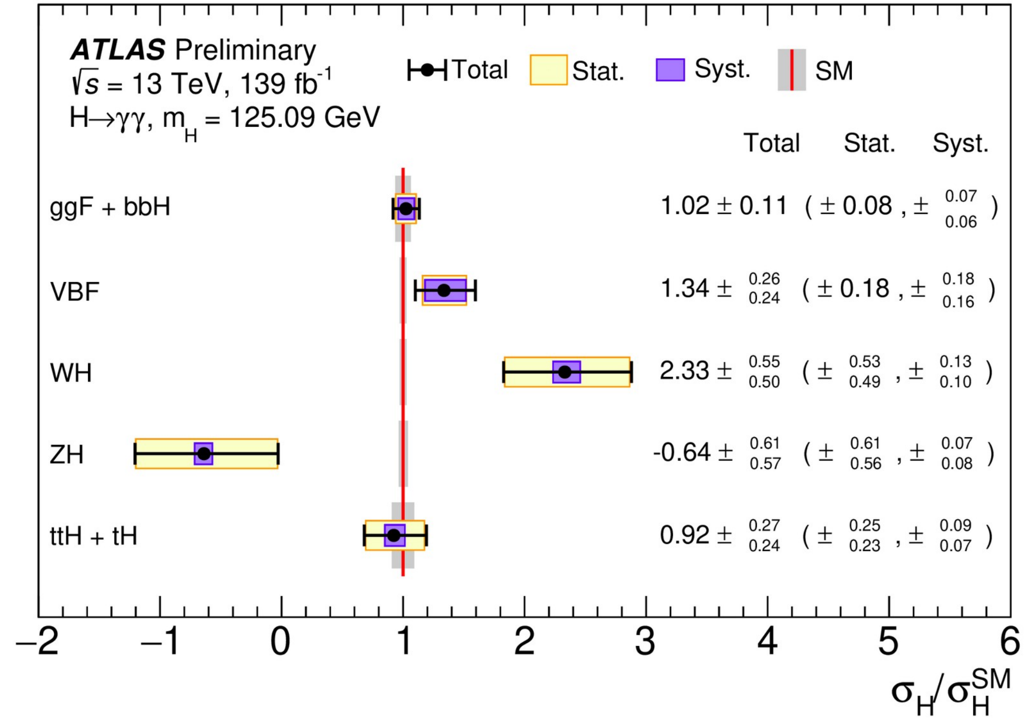

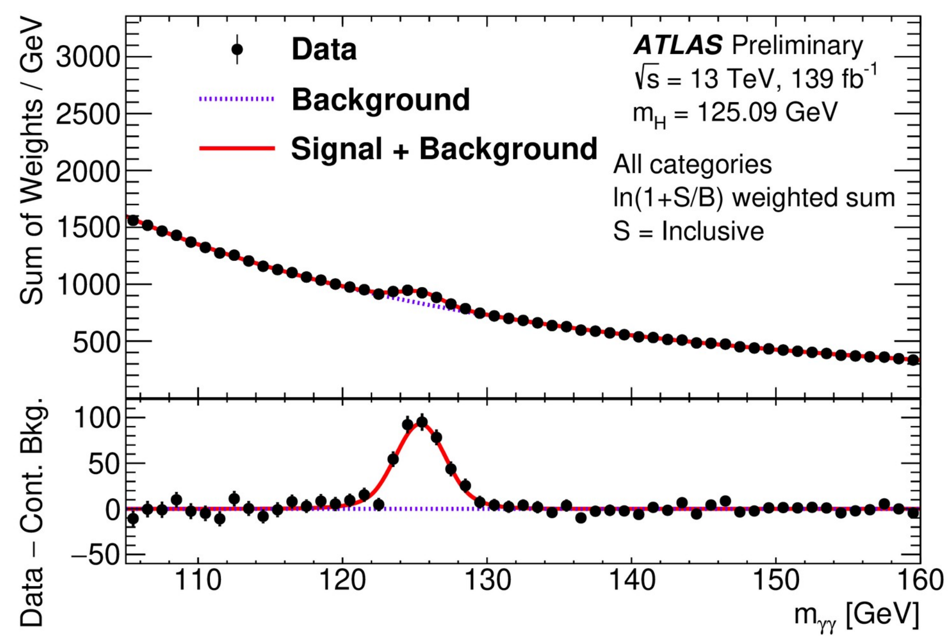

H→γγ: STXS

- Not enough statistical power to measure all stage 1.2 bins → merging down to 27 (merging scheme in back-up);
- Analysis optimized to minimize uncertainties and correlations among STXS bins;
- ~30% correlation between some VH bins (mainly due to misreconstructed leptons);
- First channel performing ttH measurements in pT_H bins;
- Upper limit of 8*SM prediction @ 95% CL set on tH production.

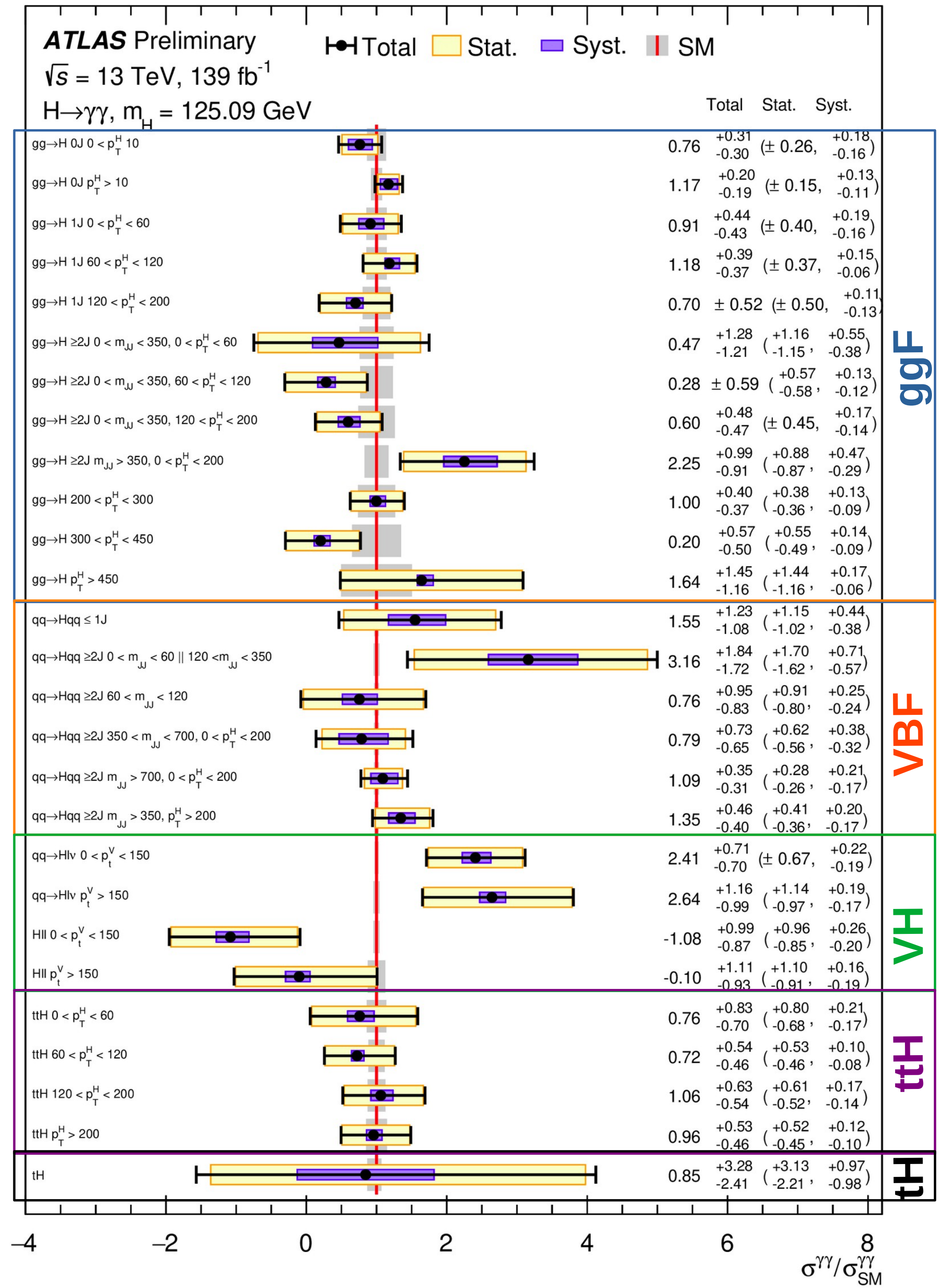

ATLAS-CONF-2020-026

H→WW: prod. mode XS

ATLAS-CONF-2021-014

- Measurements of ggF and VBF production XS and 11 STXS regions;
- Categories defined according to N_{jet} and kinematic selection targeting VBF topology;
- Multiple background sources modeled with dedicated data control regions (CRs) and Monte Carlo (MC) predictions;

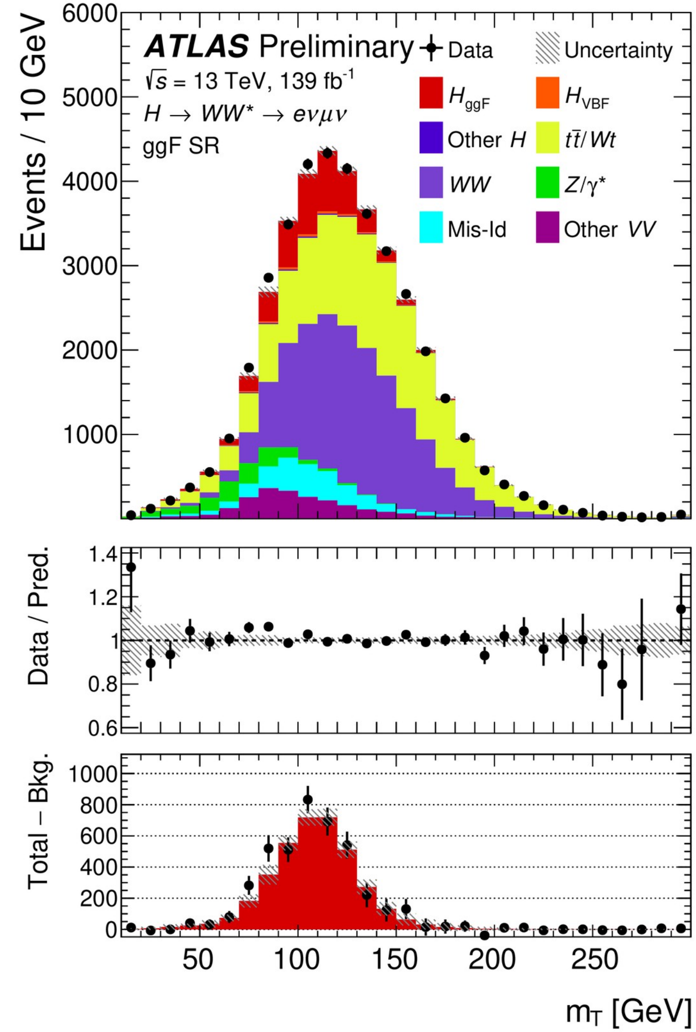

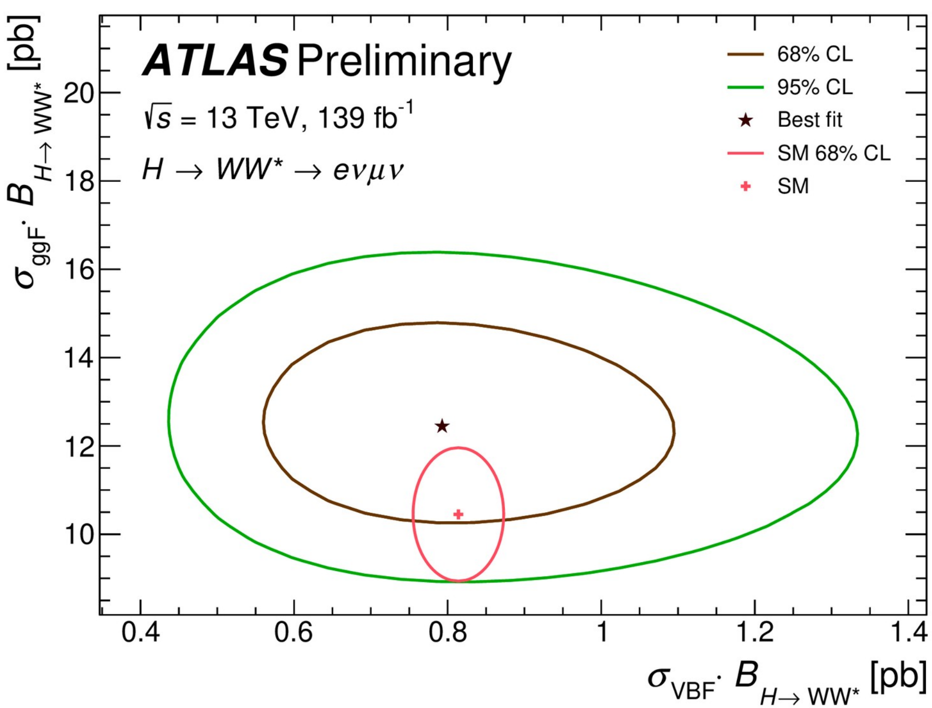

- Transverse mass of the dilepton system m_T used as observable in the fit for ggF categories;
- In the VBF category, Neural network (NN) used to separate VBF from ggF and its output used as observable.

$$m_{\mathrm{T}} = \sqrt{\left(E_{\mathrm{T}}^{\ell\ell} + E_{\mathrm{T}}^{\mathrm{miss}}\right)^2 - \left|\boldsymbol{p}_{\mathrm{T}}^{\ell\ell} + \boldsymbol{E}_{\mathrm{T}}^{\mathrm{miss}}\right|^2}$$

H→WW: STXS

- STXS measurements in 11 bins: 6 (ggF) + 5 (EW qqHqq);
- Categorization based on the prod. mode measurement with additional kinematic cuts;
- Dominant systematics: flavour tagging, missing E_T (ggF bins); jet energy scale/resolution, matrix element calculation and parton shower (ggF, VBF bins);
- Normalizations of WW and top backgrounds contribute largely to the overall uncertainty;
- The results are compatible with the SM predictions with a p-value of 52%.

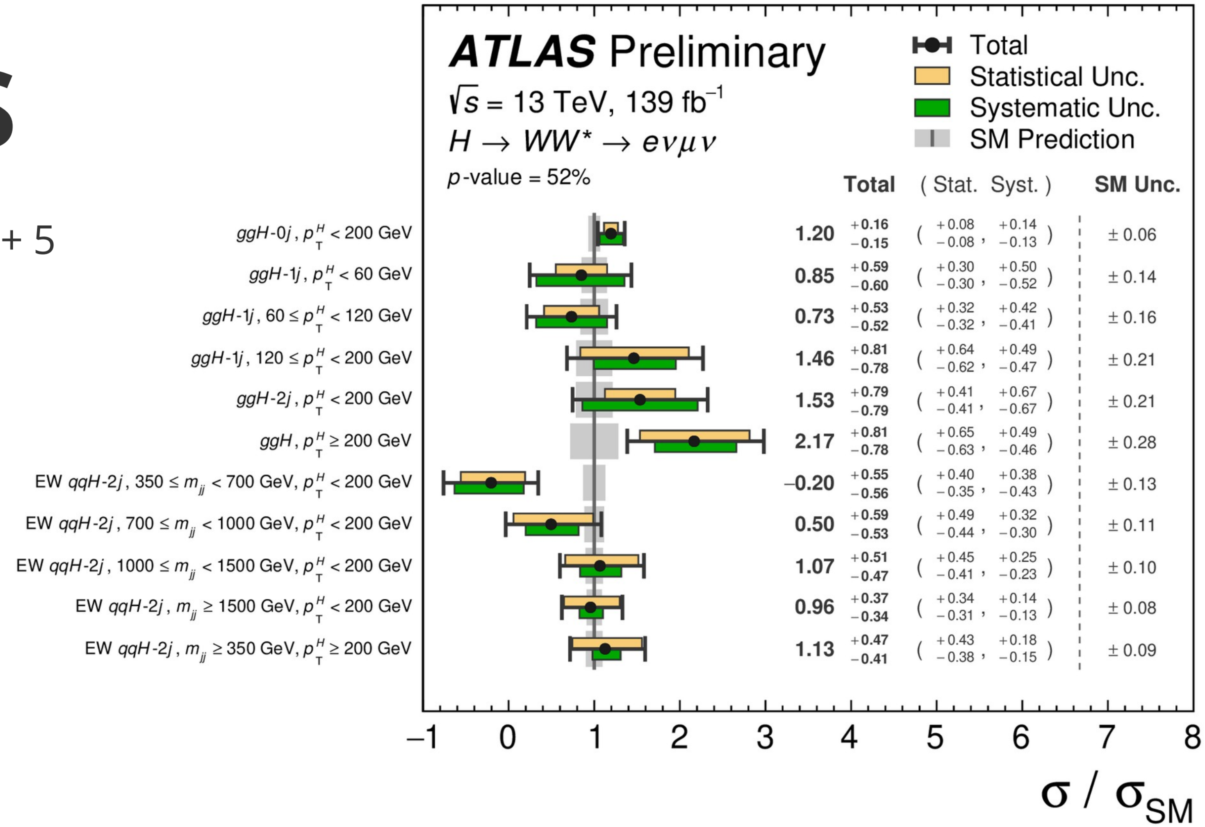

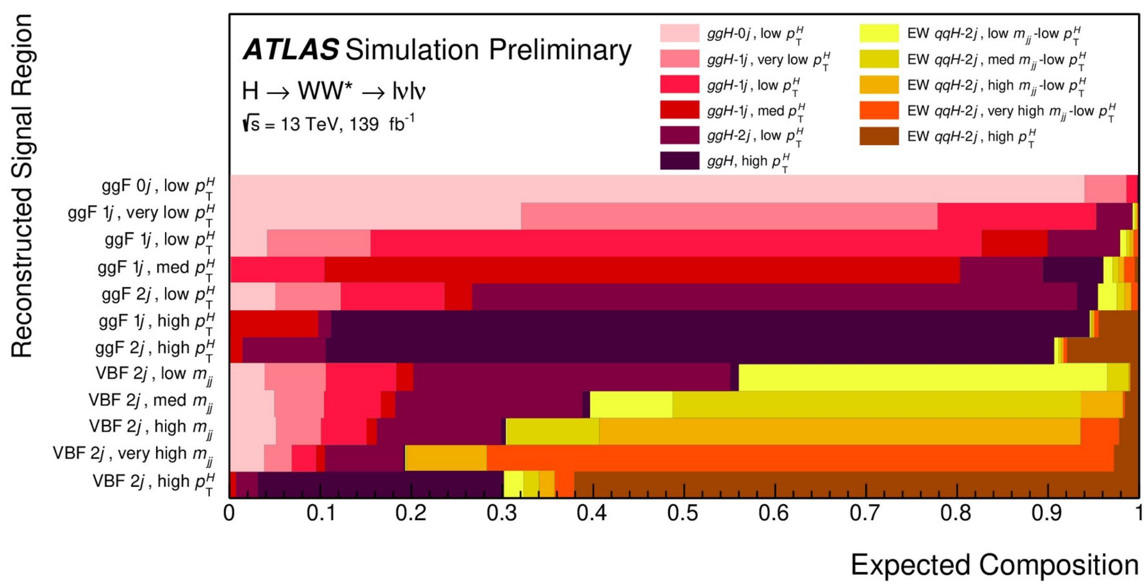

ATLAS-CONF-2021-014

H→ZZ: prod. mode XS

Eur. Phys. J. C 80 (2020) 957

- Measurements of total XS, production modes and reduced STXS 1.1 regions (12);
- Use of data sidebands to constrain the dominant ZZ non-resonant background;
- NNs used to separate different signals (e.g. ggF, VBF) and backgrounds (e.g. ZZ non-resonant) depending on the category in order to minimize the correlations among the measured XS;
- For each NN, n-1 output nodes are used as observables in the fit;
- Particle-isolation and -identification criteria optimized to retain sensitivity in the ggF regions, while increasing the efficiency for the VH and ttH categories.

$$(\sigma \times B_{H\to ZZ})_{\text{obs}} = 1.34 \pm 0.12 \text{ pb}$$

$$(\sigma \times B_{H\to ZZ})_{\text{SM}} = 1.33 \pm 0.08 \text{ pb}$$

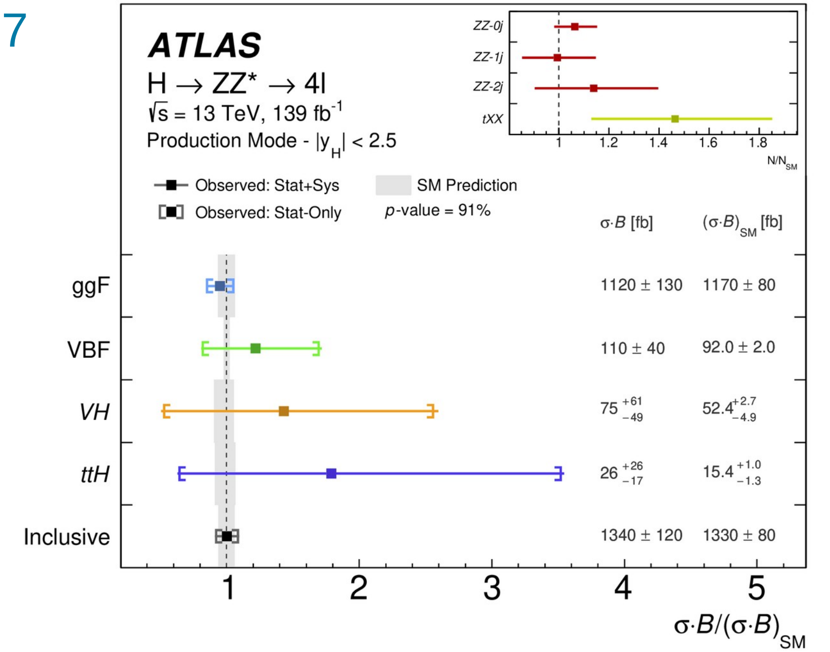

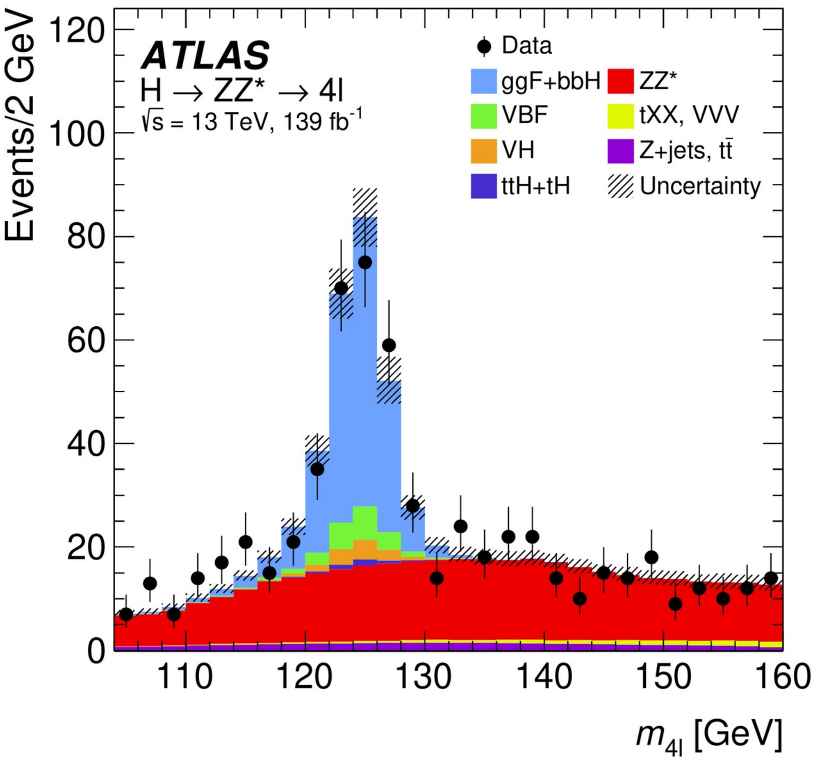

H→ZZ: STXS

- 12 Reduced Stage 1.1 bins: 6 (ggF) + 3 (EW qqH) + VH-lep + ttH;
- P-value of the compatibility test with SM is 77%;
- Additional separate measurement of an alternative qq2Hqq-VBF bin (defined by m_{jj} >350 GeV and pT_H < 200 GeV):

$0.060^{+0.025}_{-0.020}$ pb **obs**

$0.0335^{+0.0007}_{-0.0011}$ pb **SM**

20% correlation with gg2H-2j bin (due to ggF contamination in the VBF selections).

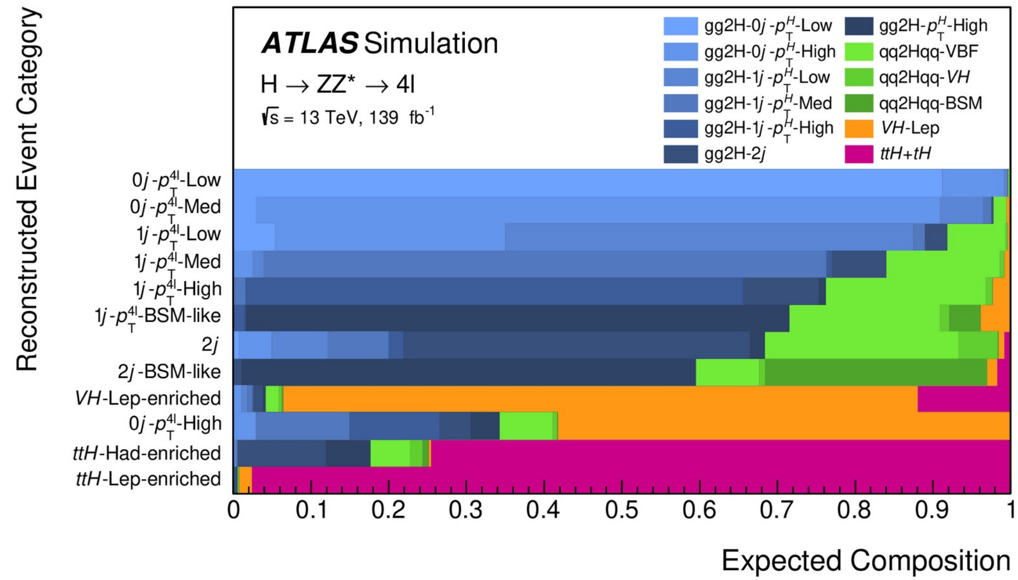

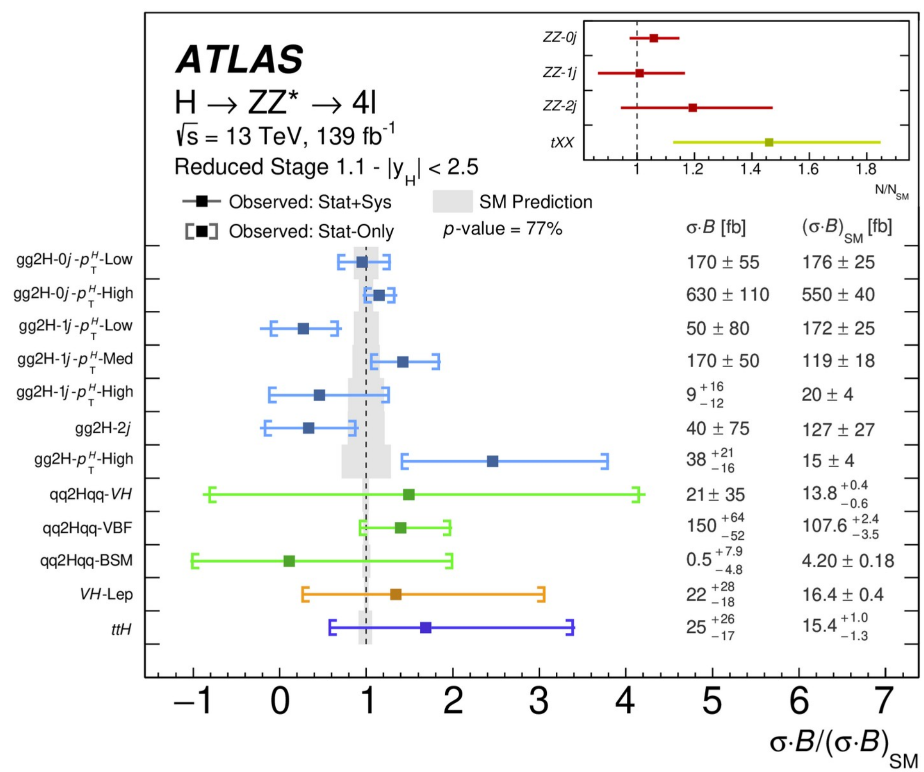

Eur. Phys. J. C 80 (2020) 957

Combination: STXS

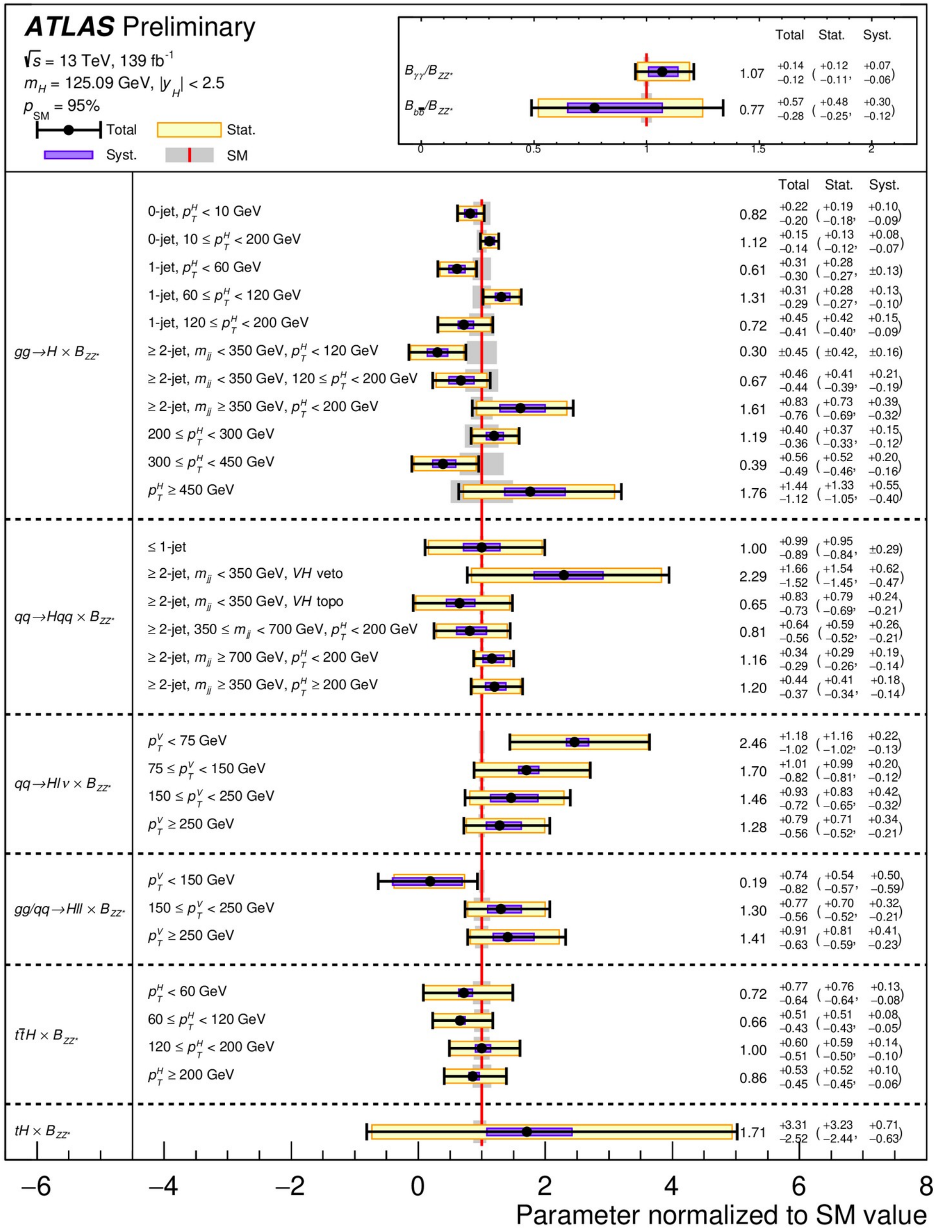

- Preliminary combined measurement of STXS Stage 1.2;
- Combination of H→γγ, H→bb (VH only), H→ZZ*→4l analyses;
  - H→WW not included yet!
- Relative uncertainties ranging from 10% to 100% (most limited by statistics);
- Compatibility level with SM: 95%;
- They are used as input for the EFT and κ interpretation;
- Reparametrization in terms of BR_{ZZ}

$$(\sigma \times B)_{if} = (\sigma \times B)_{i,ZZ} \cdot \left(\frac{B_f}{B_{ZZ}}\right)$$

κ interpretation

- Measurements of coupling-strength modifiers κ;
- Combination of H→γγ, ZZ, WW, ττ, bb, μμ, invisible;
- Using effective photon and gluon couplings κ_γ and κ_g;
- Testing with and without BSM contributions in decays (B_i invisible rate, B_u undetected rate);
- Negative value for κ_t is excluded at 2.9σ;
- The SM corresponds to $B_i = B_u = 0$ and all κ set to unity.

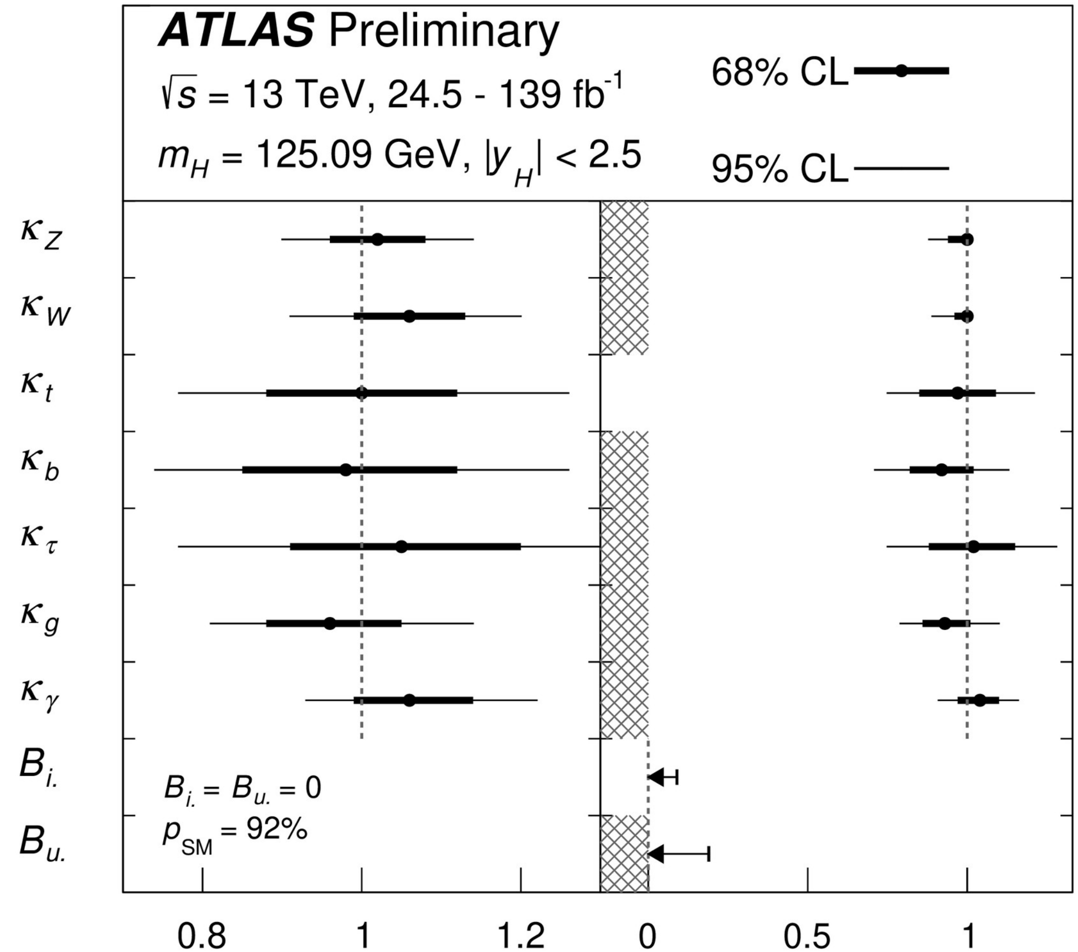

$$\sigma \cdot \mathcal{B}\,(i \to H \to f) = \kappa_i^2 \cdot \kappa_f^2 \cdot \sigma_i^{\mathrm{SM}} \cdot \frac{\Gamma_f^{\mathrm{SM}}}{\Gamma_H(\kappa_i^2, \kappa_f^2)}$$

$$\kappa_i^2 = \frac{\sigma_i}{\sigma_i^{\mathrm{SM}}} \quad \text{and} \quad \kappa_f^2 = \frac{\Gamma_f}{\Gamma_f^{\mathrm{SM}}}$$

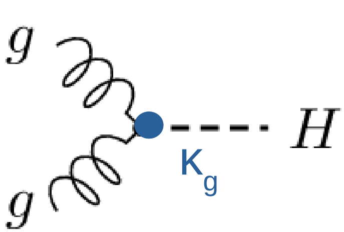

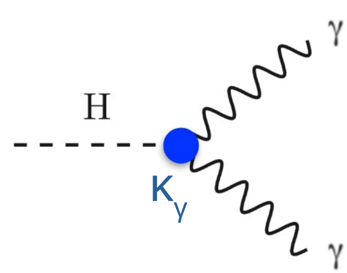

ATLAS-CONF-2020-053

EFT

Generalization of κ framework!

$$\mathcal{L}_{\mathrm{SMEFT}} = \mathcal{L}_{\mathrm{SM}} + \sum_{i}^{N_{d6}} \frac{c_i}{\Lambda^2} O_i^{(6)}$$

- The SMEFT extends the SM Lagrangian by adding new operators;
- Parametrize the STXS regions in terms of the c_i (Wilson coefficients);
- Constrain EFT coefficients → put limits on BSM theories.

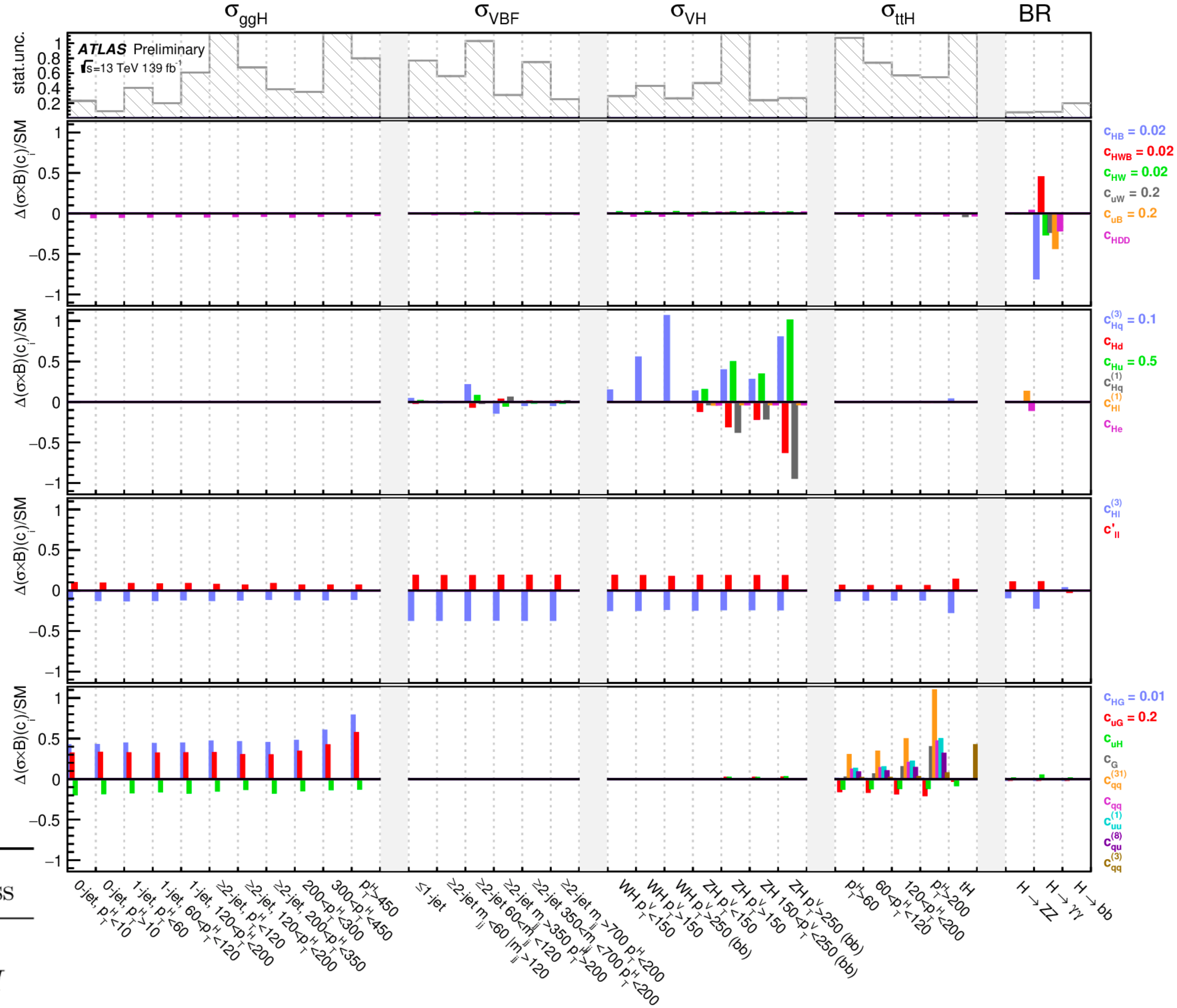

Coefficient	Operator	Example process
c_{HDD}	$(H^\dagger D^\mu H)^* (H^\dagger D_\mu H)$	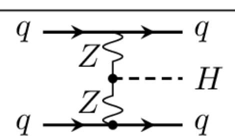
c_{HB}	$H^\dagger H\, B_{\mu\nu} B^{\mu\nu}$	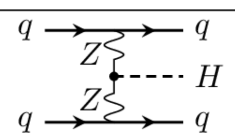
c_{HW}	$H^\dagger H\, W^I_{\mu\nu} W^{I\mu\nu}$	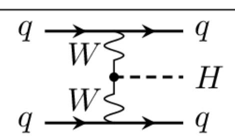
c_{HWB}	$H^\dagger \tau^I H\, W^I_{\mu\nu} B^{\mu\nu}$	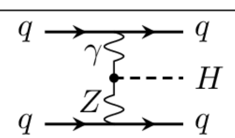

$c_{Hq}^{(3)}$	$(H^\dagger i\overleftrightarrow{D}^I_\mu H)(\bar{q}_p \tau^I \gamma^\mu q_r)$	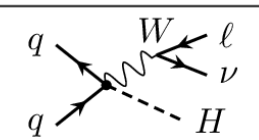
$c_{Hl}^{(1)}$	$(H^\dagger i\overleftrightarrow{D}_\mu H)(\bar{l}_p \gamma^\mu l_r)$	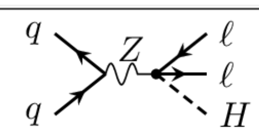
$c_{Hl}^{(3)}$	$(H^\dagger i\overleftrightarrow{D}^I_\mu H)(\bar{l}_p \tau^I \gamma^\mu l_r)$	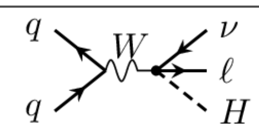

EFT results

- Cannot constrain all c_i due to limited sensitivity to certain processes;
- “Flat” directions (0 sensitivity) of the likelihood are identified via a Principal Component Analysis (PCA) and set to 0;
- Simultaneously fit combinations of c_i selected according to expected sensitivity;
- Using SMEFT linearized model and model including quadratic terms;
- Due to the selection of the H→4l analysis, SMEFT operators affect the acceptance → taken into account with the application of a correction function;
- All measured c_i are compatible with 0 (SM prediction).

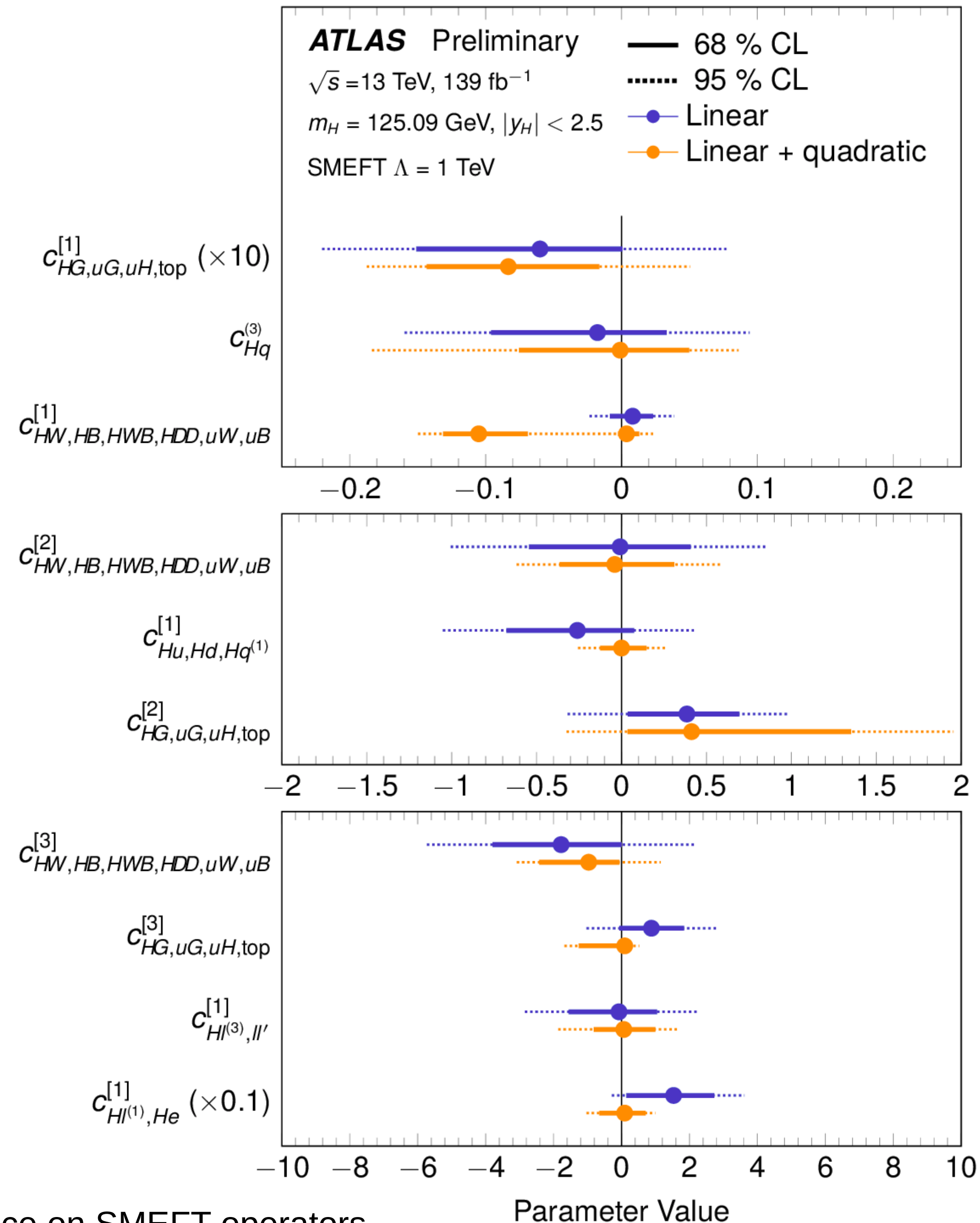

$$|M_{SM} + c_i M_{SMEFT,i}|^2$$

$$\sigma_{\text{STXS}} = \sigma_{\text{SM}} + \sigma_{\text{int}} + \sigma_{\text{BSM}}$$

Linear dependence on SMEFT operators

Quadratic dependence

H→WW + WW (SM): EFT

ATL-PHYS-PUB-2021-010

L=36.1fb^{-1}

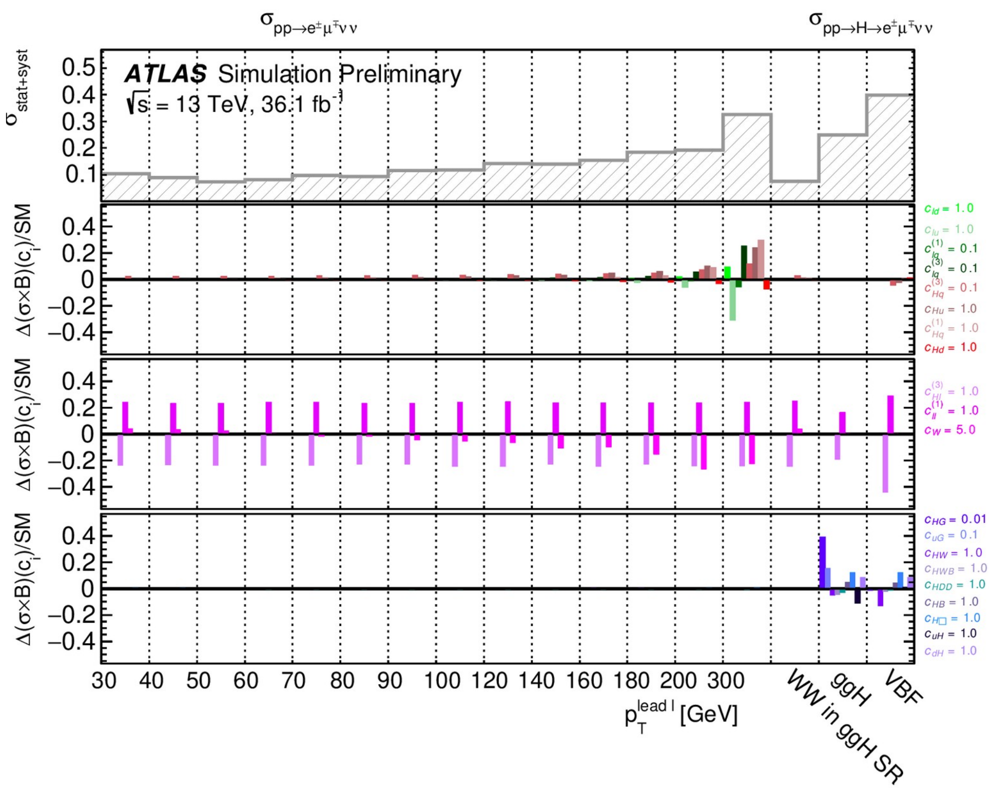

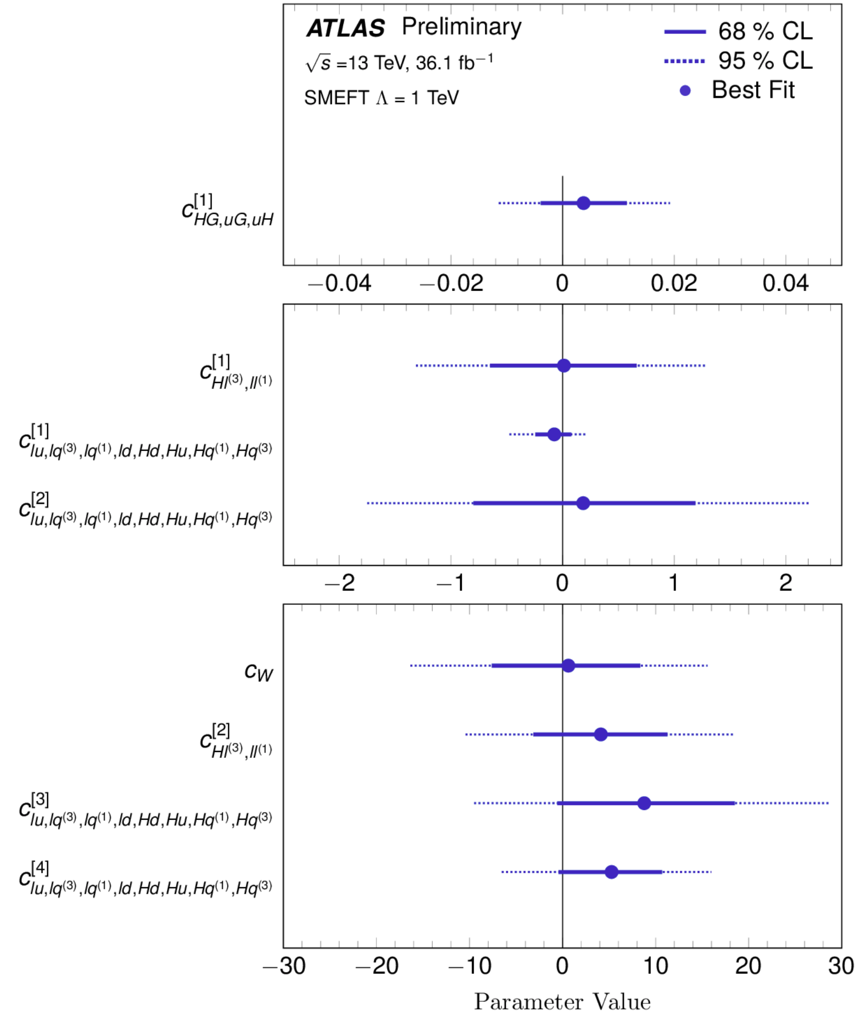

- Measurements of ggF and VBF signal strenghts in H→WW + differential XS of WW production in the 0-jet channel;
- Parametrization of the WW background in terms of EFT operators;
- Consider impact of 20 EFT operators → PCA reduction → simultaneous fit on 8 combinations;
- O_{HW} and $O_{HI}^{(3)}$ operators influence the Higgs decay kinematics leading to acceptance effects in ggF region → taken into account with a correction factor;
- **First step towards a global EFT fit!**

- Including other areas (e.g. SM electroweak, top quark) in the combination → constrain more EFT parameters.

Higgs self-coupling in HH→γγbb

- Constrain Higgs boson trilinear coupling modifier κ_λ using non-resonant di-Higgs (HH) production;
- Divide events in $m_{\gamma\gamma bb}$ < 350 GeV and $m_{\gamma\gamma bb}$ > 350 GeV to improve sensitivity to κ_λ variations;
- Use BDTs to reject backgrounds (non-resonant γγ, single H);
- Fit $m_{\gamma\gamma}$ using analytic models for signal and background;
- Upper limit of 4.1*SM prediction @ 95% CL set on HH production;
- Limit on κ_λ is [-1.5, 6.7] @ 95% CL ;

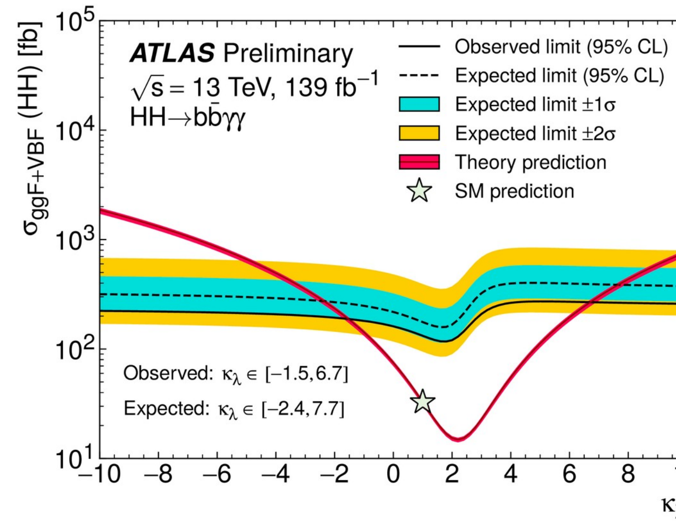

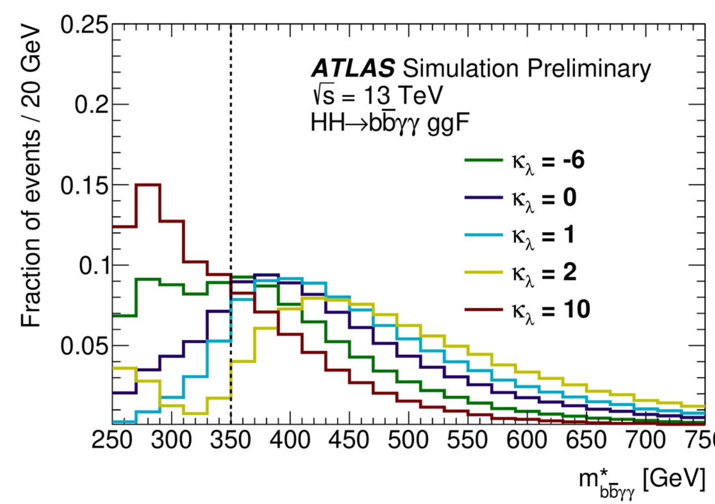

$$\kappa_\lambda = \lambda_{HHH} / \lambda_{HHH}^{\text{SM}}$$

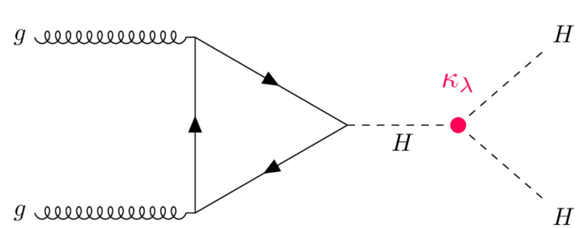

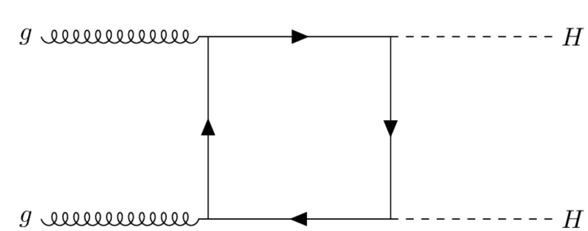

Rare decays: H→γ*(→ll)γ and H→Z(→ll)γ

arXiv:2103.10322

Phys. Lett. B 809 (2020) 135754

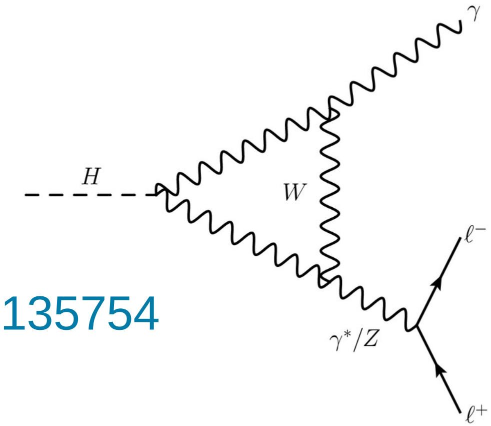

- First evidence for the decay of the Higgs boson into a pair of leptons (ee or μμ) and a photon: 3.2σ (H→γ*γ);
- Experimental challenge: low m_{ll} → leptons are collimated;

- Upper limit @95%CL set on pp→H→Zγ XS times BR: 3.6*SM prediction;
- Corresponding to a 2.2σ significance;

$$\mu = 1.5 \pm 0.5$$

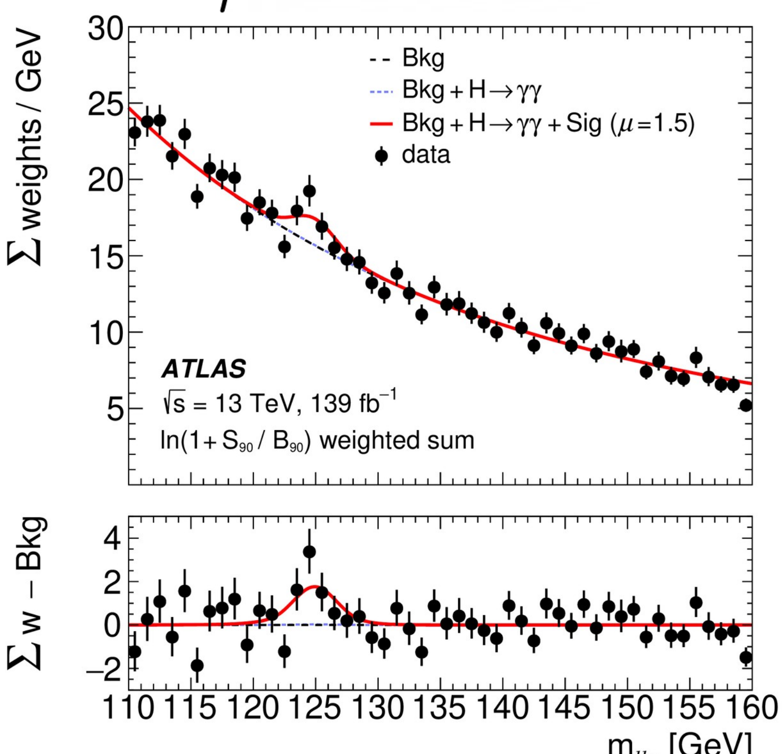

$$\mu = 2.0^{+1.0}_{-0.9}$$

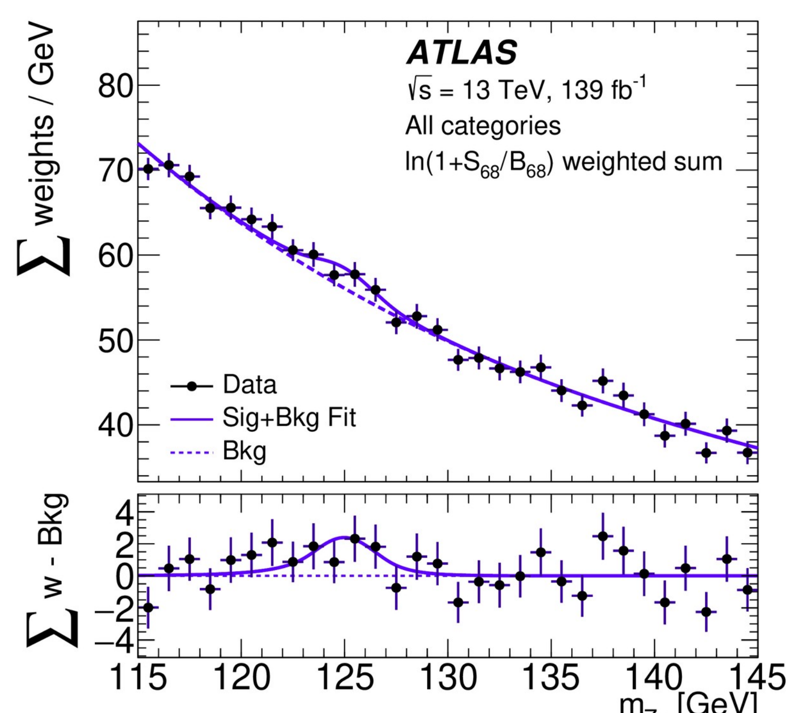

Higgs CP properties

Phys. Rev. Lett. 125 (2020) 061802

$$\mathcal{L} = -\frac{m_t}{v}\{\bar{\psi}_t\kappa_t[\cos(\alpha) + i\sin(\alpha)\gamma_5]\psi_t\}H$$

Top Yukawa coupling — CP-mixing angle

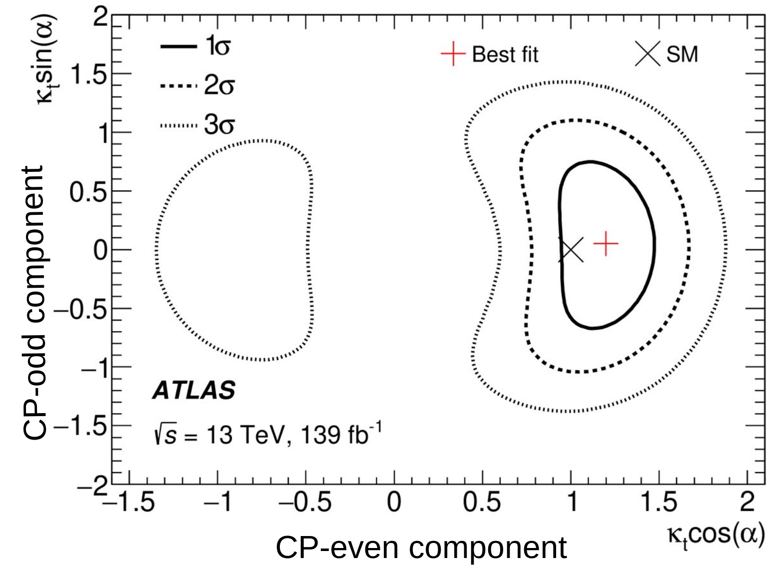

- Higgs CP tested with ttH/tH productions and H→γγ decays;
- Pure CP-odd excluded at 3.9σ and |α|>43° excluded at 95% CL.

$$\mathcal{L}_0^{\mathrm{loop}} = -\frac{1}{4}\left(\kappa_{Hgg}g_{Hgg}G^a_{\mu\nu}G^{a,\mu\nu} + \kappa_{Agg}g_{Hgg}G^a_{\mu\nu}\tilde{G}^{a,\mu\nu}\right)H$$

= 0 in the SM

$$\kappa_{Agg}/\kappa_{Hgg} = 0.0 \pm 0.4(\mathrm{stat.}) \pm 0.3(\mathrm{syst.})$$

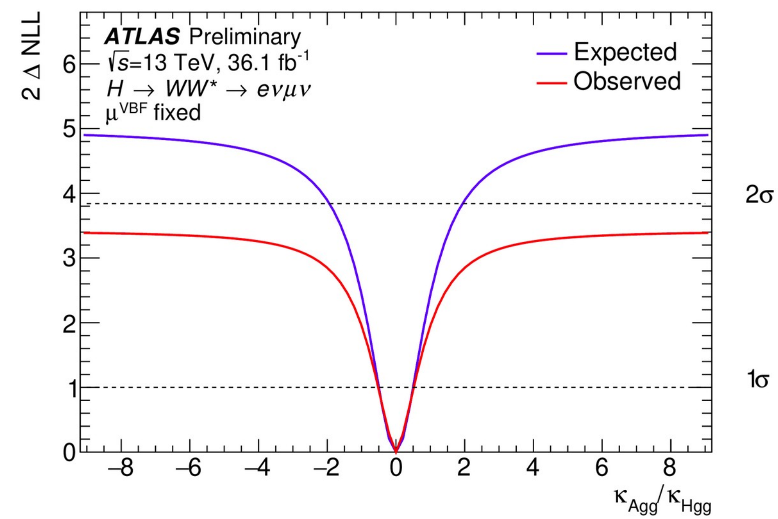

- CP structure of (effective) coupling to gluons tested with H→WW events in the ggF+2jets channel;
- Polarisation of the HVV couplings tested in the VBF channel (results consistent with the SM).

ATLAS-CONF-2020-055 L=36.1ifb

Conclusions

- Many interesting results produced by ATLAS using Run 2 data;
- Higgs properties studied using key (in particular bosonic) decay channels;
- All measurements are in good agreement with the SM;
- Interpretation through the most advanced frameworks → no hint of new physics observed;
- Outlook:
  - Expect more results with full Run 2 data;
  - Combination ATLAS+CMS;
  - Improvements of analysis methods;
  - Expect improvement from the larger datasets of Run 3 (x2) and especially HL-LHC (x20).

BACK-UP

H→ZZ: neural network

- Neural Neworks (NNs) consists of two recurrent networks (one related to the 4 leptons and one related to jets) in combination with a multilayer perceptron (containing info related to full event);
- Input variables per category:

Category	Processes	MLP	Lepton RNN	Jet RNN	Discriminant
$0j$-$p_T^{4\ell}$-Low $0j$-$p_T^{4\ell}$-Med	ggF, ZZ^*	$p_T^{4\ell}$, D_{ZZ^*}, m_{12}, m_{34}, $\lvert\cos\theta^*\rvert$, $\cos\theta_1$, ϕ_{ZZ}	p_T^ℓ, η_ℓ	-	NN_{ggF}
$1j$-$p_T^{4\ell}$-Low	ggF, VBF, ZZ^*	$p_T^{4\ell}$, p_T^j, η_j, $\Delta R_{4\ell j}$, D_{ZZ^*}	p_T^ℓ, η_ℓ	-	NN_{VBF} for $NN_{ZZ} < 0.25$ NN_{ZZ} for $NN_{ZZ} > 0.25$
$1j$-$p_T^{4\ell}$-Med	ggF, VBF, ZZ^*	$p_T^{4\ell}$, p_T^j, η_j, E_T^{miss}, $\Delta R_{4\ell j}$, D_{ZZ^*}, $\eta_{4\ell}$	p_T^ℓ, η_ℓ	-	NN_{VBF} for $NN_{ZZ} < 0.25$ NN_{ZZ} for $NN_{ZZ} > 0.25$
$1j$-$p_T^{4\ell}$-High	ggF, VBF	$p_T^{4\ell}$, p_T^j, η_j, E_T^{miss}, $\Delta R_{4\ell j}$, $\eta_{4\ell}$	p_T^ℓ, η_ℓ	-	NN_{VBF}
$2j$	ggF, VBF, VH	m_{jj}, $p_T^{4\ell jj}$	p_T^ℓ, η_ℓ	p_T^j, η_j	NN_{VBF} for $NN_{VH} < 0.2$ NN_{VH} for $NN_{VH} > 0.2$
$2j$-BSM-like	ggF, VBF	η_{ZZ}^{Zepp}, $p_T^{4\ell jj}$	p_T^ℓ, η_ℓ	p_T^j, η_j	NN_{VBF}
VH-Lep-enriched	VH, ttH	N_{jets}, $N_{b\text{-jets},70\%}$, E_T^{miss}, H_T	p_T^ℓ	-	NN_{ttH}
ttH-Had-enriched	ggF, ttH, tXX	$p_T^{4\ell}$, m_{jj}, $\Delta R_{4\ell j}$, $N_{b\text{-jets},70\%}$,	p_T^ℓ, η_ℓ	p_T^j, η_j	NN_{ttH} for $NN_{tXX} < 0.4$ NN_{tXX} for $NN_{tXX} > 0.4$

$H\to\gamma\gamma$: categorization

- IDEA: Targets the full STXS granularity simultaneously. Optimized for the determinant of the covariance matrix of the results, it takes into accounts both errors and correlations of the fit.
- PROCEDURE:
  - Train a multiclass BDT over 44 STXS truth bins (signal only) with high level and top-reco variables;
  - D-optimality: weight the multiclass outputs and classify events in 44 reco classes;
  - In each reco class, train a binary BDT (signal vs backgrounds) with high level and top-reco variables;
  - Build 88 categories with significance scans over BDT outputs

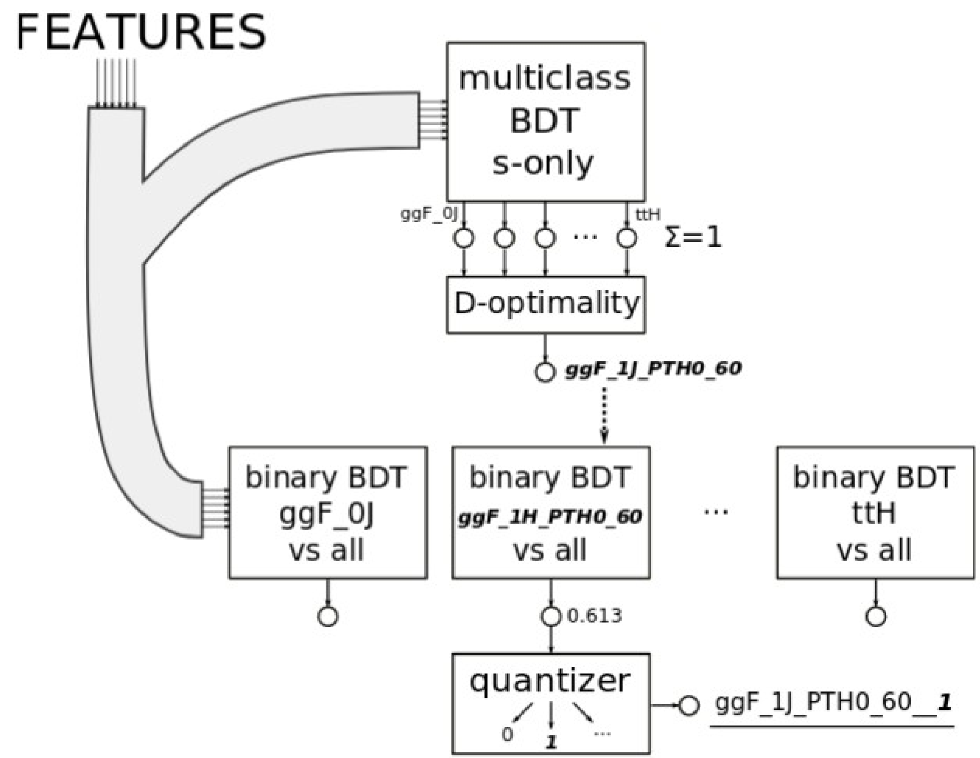

H→γγ: STXS merging

- Not enough statistical power to fit all 44 → merge down to 27 bins.

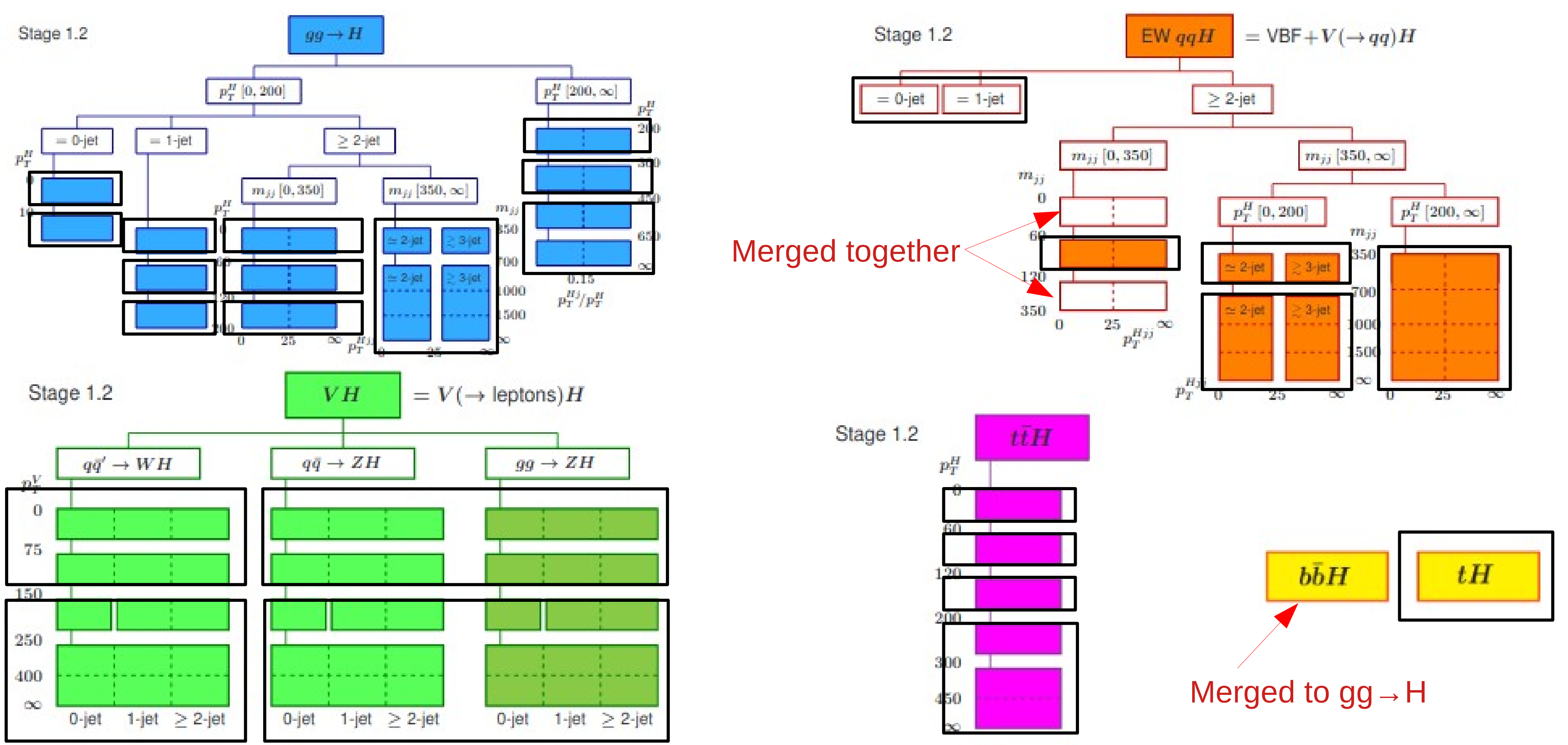

ATLAS-CONF-2020-055

L=36.1ifb

Polarisation-dependent couplings in VBFH(→WW)

- In the SM, HVV couplings are insensitive to polarisations (κ_{VV}=1, ε_{VV}=0);
- Exploiting both production and decay and assuming CP-even Higgs;
- Using rate and shape information from the $\Delta\varphi_{jj}$ distribution.

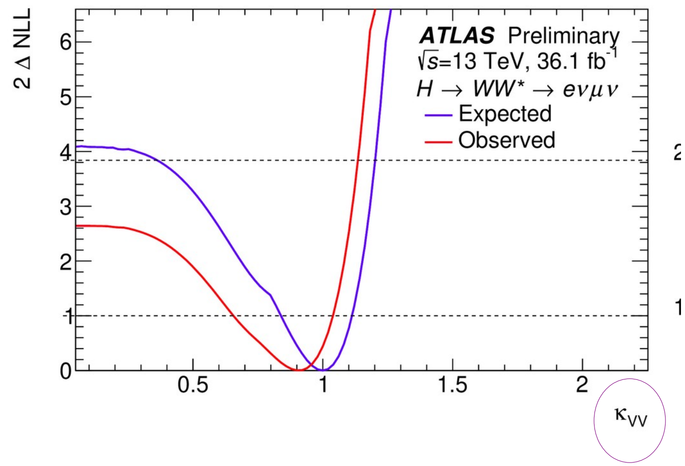

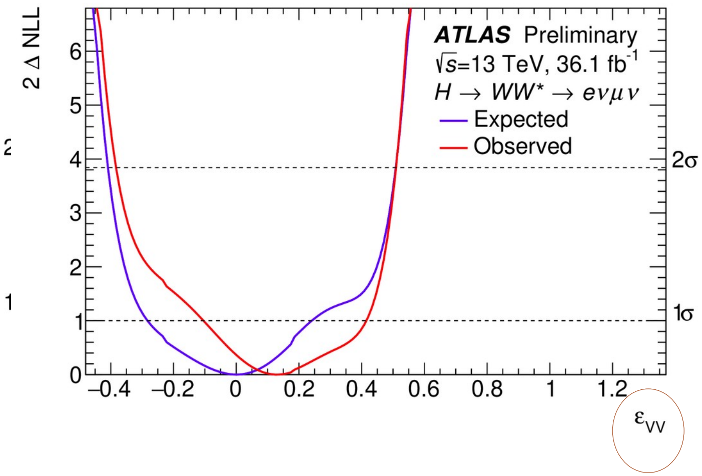

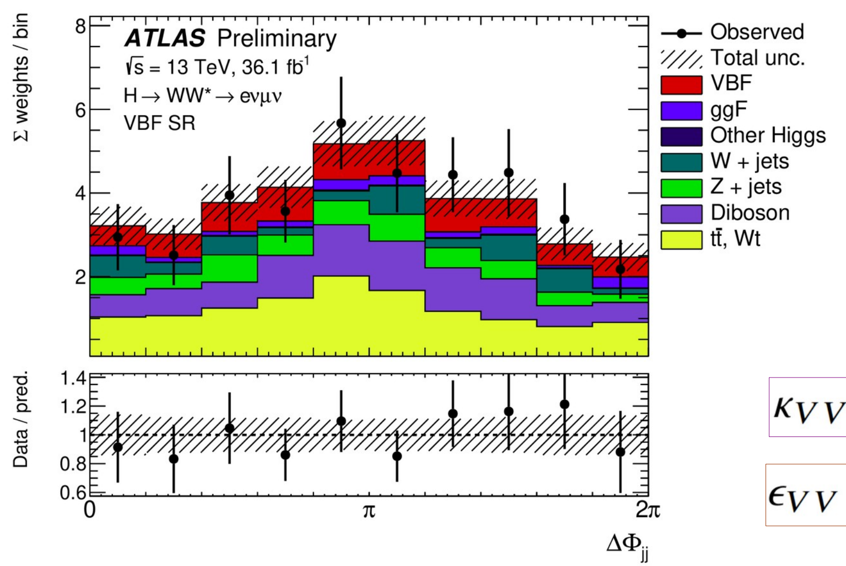

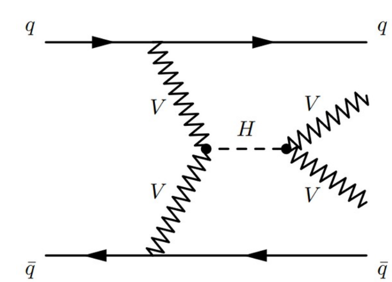

$$\kappa_{VV} = 0.90^{+0.10}_{-0.18}(\text{stat.})^{+0.09}_{-0.16}(\text{syst.})$$

$$\epsilon_{VV} = 0.13^{+0.28}_{-0.20}(\text{stat.})^{+0.08}_{-0.10}(\text{syst.})$$

$$\mathcal{L} = \kappa_{VV}\left(\frac{2m_W^2}{v}HW_\mu^+W^{-\mu} + \frac{m_Z^2}{v}HZ_\mu Z^\mu\right) - \frac{\varepsilon_{VV}}{2v}\left(2HW_{\mu\nu}^+W^{-\mu\nu} + HZ_{\mu\nu}Z^{\mu\nu} + HA_{\mu\nu}A^{\mu\nu}\right)$$

Combination: prod. mode and BR

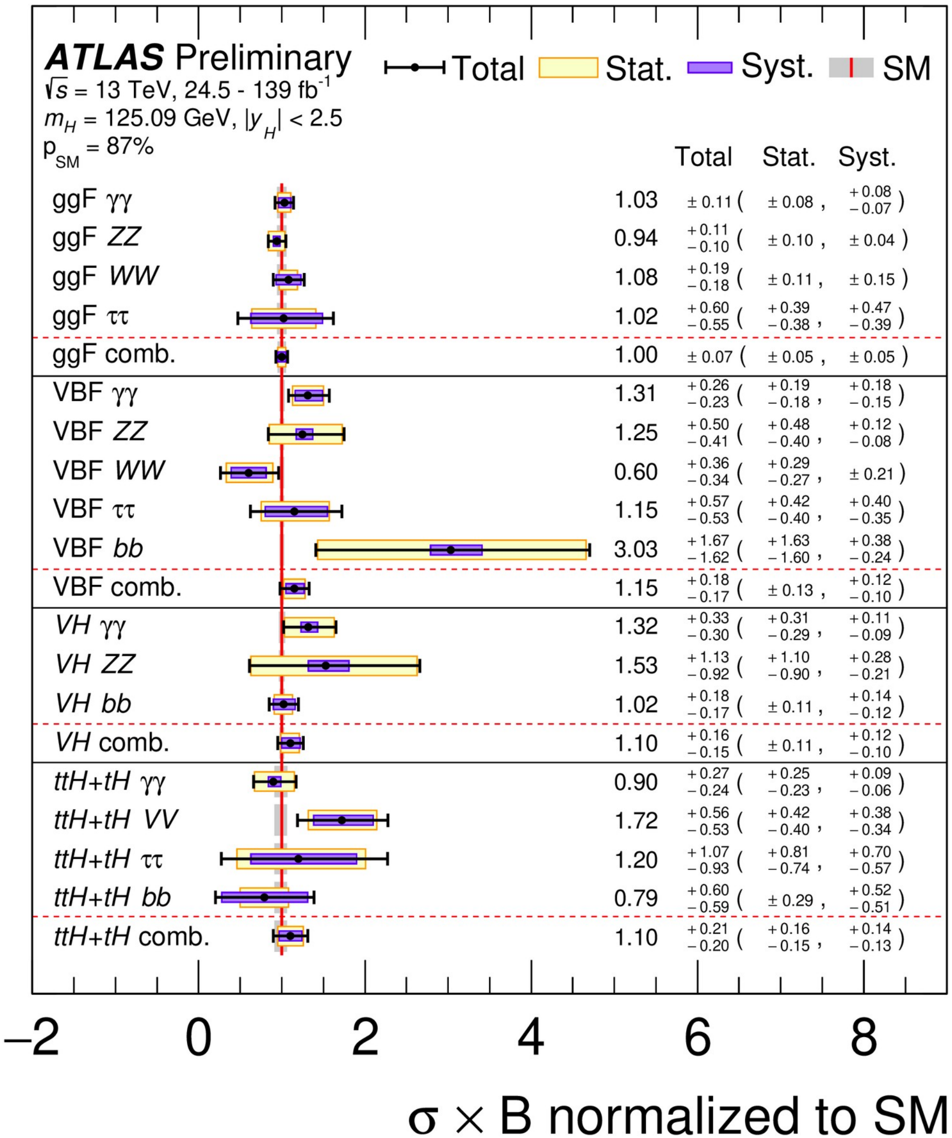

- Measurements of cross section times branching ratio per decay channel and per production mode (also combined) normalized to their SM prediction;
- The cross sections of the ggF(H→ b$\bar{b}$), VH(H → WW*) and VH(H→ττ) processes are fixed to their SM predictions;
- Compatibility level with SM: 87%;

EFT: choice of measured parameters

- It's not possible to fit/constrain all the c_i → must find the optimal set through a Principal Component Analysis;
- C_{STXS} is the SM expected covariance matrix of the measurement; P is the linearised parametrisation matrix;
- C^{-1}_{EFT} represents (Gaussian approx.) the Fisher information matrix of its SMEFT re-parametrisation;
- Eigenvalue decomposition of C^{-1}_{EFT} → eigenvectors corresponding to the most sensitive directions.

ATLAS Preliminary $\sqrt{s}$ = 13 TeV, 139 fb^{-1}

$$C^{-1}_{\mathrm{EFT}} = P^{\top} C^{-1}_{\mathrm{STXS}} P$$

#	λ	$c_{Hq}^{(3)}$	c_{HB}	c_{HW}	c_{HWB}	c_{uB}	c_{uW}	c_{HDD}	c_{Hd}	c_{Hu}	$c_{Hq}^{(1)}$	c_{He}	$c_{Hl}^{(1)}$	$c_{Hl}^{(3)}$	$c_{ll}^{(1)}$	c_{HG}	c_{uG}
1	299310		-0.70	-0.23	0.39	-0.04	-0.02									0.55	0.02
2	121830		-0.47	-0.15	0.26	-0.03										-0.83	-0.03
3	1960	0.99		0.10	0.03				-0.03	0.09	-0.05			-0.02	0.02		
4	38	-0.11	0.09		0.15			0.02	-0.26	0.84	-0.41	-0.02	-0.02	-0.06	0.04		0.08
5	19		0.10	-0.19	0.06					0.03	-0.02	-0.07	0.09	-0.13	0.10	0.02	-0.69
6	10	0.08		-0.57	-0.34			-0.02	-0.02	0.08	-0.10	0.13	-0.13	0.54	-0.40		-0.04
7	5.9	-0.07	-0.23	0.73		-0.03	-0.02	-0.03	-0.02	0.08		0.10	-0.15	0.44	-0.25		-0.13
8	1.1	-0.01	-0.02	0.08				-0.02	-0.02	0.04	-0.02	-0.01	0.02	0.08	-0.03	0.03	-0.68
9	0.3	-0.02	-0.41	0.09	-0.70	-0.02	-0.01	-0.12	0.01	-0.03	-0.36	0.16		-0.37	0.10		-0.05
10	0.16		0.09	-0.09	0.09	-0.04	-0.01	-0.04		0.10	0.31	0.29	-0.58	-0.26	-0.12		-0.07
11	0.036		0.03	0.03	0.07	-0.01	0.04	0.19	-0.04		0.03	0.09	-0.06	-0.18	-0.07	0.01	-0.16
12	0.023		-0.01				0.37	-0.01		-0.01	-0.03	-0.02	0.03	0.05	0.03		0.01

#	λ	c_{G}	$c_{qd}^{(8)}$	$c_{qq}^{(1)}$	c_{qq}	$c_{qq}^{(3)}$	$c_{qq}^{(31)}$	$c_{qu}^{(1)}$	$c_{qu}^{(8)}$	c_{uH}	$c_{ud}^{(8)}$	c_{uu}	$c_{uu}^{(1)}$	$c_{H\Box}$	c_{dH}	c_{W}	c_{eH}
1	299310															-0.02	
2	121830																
3	1960																
4	38									0.02				0.03			
5	19	0.17	0.03	0.03	0.22	0.05	0.52		0.15	-0.08	0.03	0.02	0.23	0.07	0.06		
6	10				0.02		0.04			-0.02			0.02	-0.20	-0.08		
7	5.9	0.08			0.09	0.02	0.22		0.06				0.10	-0.07	-0.11		
8	1.1	-0.29	-0.03	-0.04	-0.24	-0.04	-0.52	-0.01	-0.15	-0.10	-0.03	-0.02	-0.25	0.04			
9	0.3	0.03								0.06				0.06	-0.11	-0.01	
10	0.16	0.02				-0.04				0.08				0.27	-0.52	-0.02	0.01
11	0.036	0.22	-0.01	0.01	-0.01	-0.10	-0.09		-0.02	0.70	-0.01		-0.02	-0.56	0.09		-0.02
12	0.023	-0.05			0.03	-0.91	0.08		0.02	-0.02			0.03	0.09			

CP structure of tH/ttH(→γγ)

$$\mathcal{L} = -\frac{m_t}{v}\{\bar{\psi}_t\kappa_t[\cos(\alpha) + i\sin(\alpha)\gamma_5]\psi_t\}H$$

Top Yukawa coupling   CP-mixing angle

- The SM predicts a CP-even (α=0) Higgs boson;
- ttH and tH productions are sensitive to deviations from SM couplings;
- Background rejection and CP-odd(even) separation using two BDTs;
- κ_γ and κ_g constrained by the results obtained in the combination;
- Pure CP-odd excluded at 3.9σ and |α|>43° excluded at 95% CL.

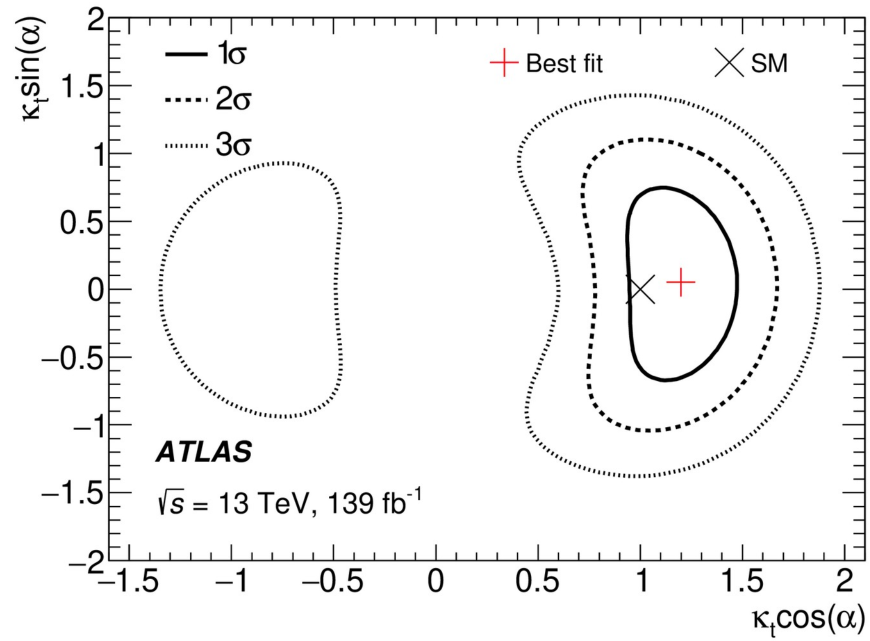

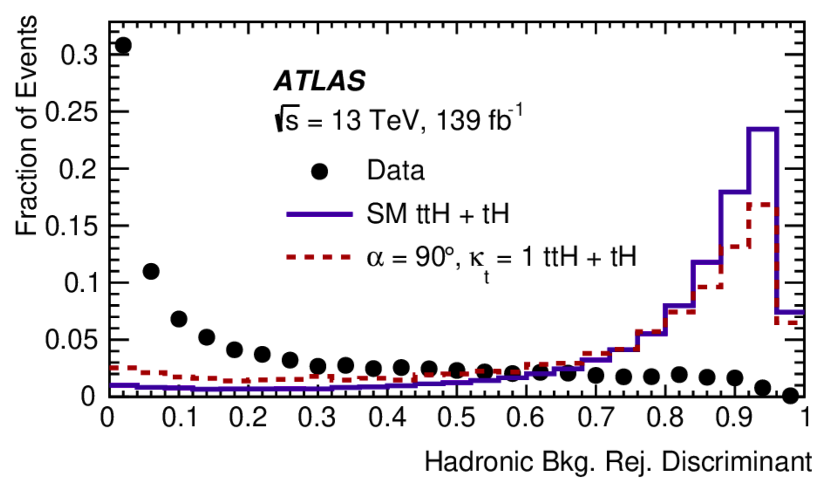

Eur. Phys. J. C 80 (2020) 957

EFT: H→4l acceptance effect

- H→ZZ→4l analysis has reconstruction level selection on m_{12} and m_{34} to target the signal;
- Large impact on EFT signal acceptance and on c_i limit;
- 3D (c_{HW}, c_{HB}, c_{HWB}) Lorentz function used to model a correction factor;